

# Precipitation of vanadium carbide in an Ni-38 at.% Fe 3 at.% V-2.4 at.% C alloy

R. B. SCARLIN

*Brown-Boveri Research Centre, 5401 Baden, Switzerland*

J. W. EDINGTON

*Department of Metallurgy and Materials Science, University of Cambridge, UK*

An electron microscopy investigation of the precipitation of vanadium carbide in a nickel-iron base alloy is reported. Three types of precipitate occur, matrix-dot, stacking fault and secondary precipitate depending upon ageing time and temperature. The morphology identity, and orientation relationships of the secondary precipitate have been determined. The features of matrix-dot precipitate free and enhanced zones have been studied, and a mechanism is proposed to explain the latter.

## 1. Introduction

The precipitation of fine coherent (MC) transition metal carbide particles has been frequently used as a method of strengthening stainless steels and cobalt alloys. Precipitation has been observed on stacking faults and unit dislocations together with homogeneously distributed matrix-dot precipitation depending on the ageing temperature and time [1, 2]. For the case of matrix-dot precipitation it has been shown that both precipitate-free zones (pfz) [1] and precipitate enhanced zones (pez) [2] may form near grain boundaries. However, in all previous studies interpretation of these features was complicated by the precipitation of chromium-rich  $M_{23}C_6$  carbides at grain boundaries, which superimposed an additional composition gradient in this region. This factor was not present in the work described here.

## 2. Experimental

Stock material, prepared by vacuum-arc melting high purity materials, was solution treated *in vacuo* at 1340°C for 24 h, and then extruded and rolled at 1000°C to 12 mm square section bar. The surface decarburized layer was removed by mechanical grinding, and chemical analysis indicated a final composition of 56.4 at. % Ni, 38.2 at. % Fe, 3.04 at. % V, and 2.40 at. % C. Slices 0.25 mm in thickness were cut transversely from the bar and sealed in silica capsules under high purity argon. All material was solution

treated for two hours at  $1340 \pm 5^\circ\text{C}$ , unless otherwise stated, and rapidly quenched by breaking the capsule under water. Specimens were subsequently pre-aged or aged under argon at temperatures in the range 450 to 950°C for times up to 500 h then water quenched. Thin foils prepared by electropolishing [3] were examined by transmission electron microscopy using either a Phillips EM 300 at 100 kV or a JEM 200A at 200 kV.

## 3. Results and discussion

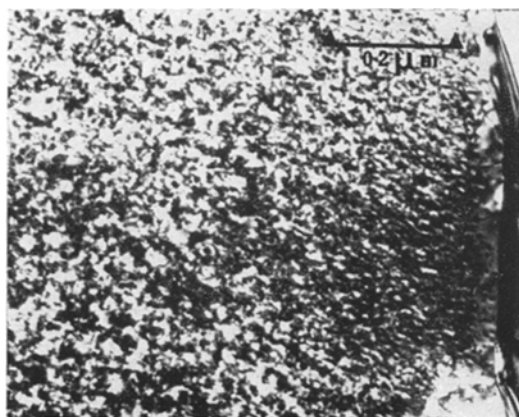
Except where specified, the precipitate identified by selected-area diffraction was always the fundamental form of vanadium carbide with the sodium chloride unit cell and lattice parameter 0.415 nm.

Grain-boundary precipitate was always observed at all stages of ageing. Within the grains the most common precipitate was matrix-dot of the type previously reported in austenite [2, 4, 5] nickel [6] cobalt [7] and nickel-iron base alloys [8]. This precipitate formed homogeneously on ageing between 600 and 925°C with particle edge lengths in the range 3 to 20 nm depending upon time and temperature [9]. At the same time stacking fault precipitation of the form described previously by several workers [2, 10] also occurred on ageing in the temperature range 600 to 800°C. For this precipitate there was an incubation time ranging from > 2 h at 600°C to < 30 min at 800°C. Both precipitates exhibited

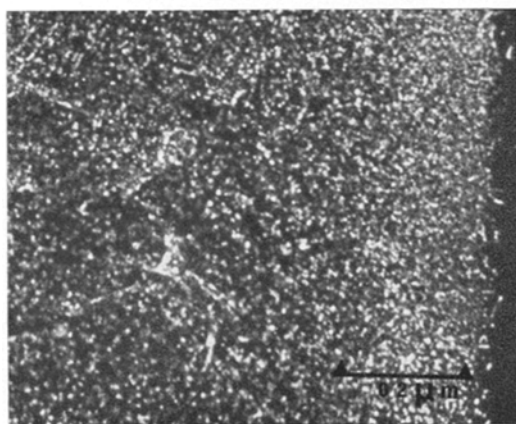
grain boundary pfz: for matrix-dot the half-width was  $\sim 0.2 \mu\text{m}$  increasing to  $0.8 \mu\text{m}$  with increased ageing temperature, while that for the stacking fault precipitate was constant at  $\sim 1 \mu\text{m}$ . Similar pfz have been reported for both types of precipitate in austenite by Froes *et al.* [1].

### 3.1. Enhanced matrix-dot precipitation

If the material is pre-aged at  $450$  to  $500^\circ\text{C}$  and aged at  $600^\circ\text{C}$  after quenching from  $\sim 1250^\circ\text{C}$ , a narrow pfz (halfwidth  $0.04$  to  $0.08 \mu\text{m}$ ) forms, see Fig. 1a, surrounded by an enhanced zone of



(a)



(b)

Figure 1 (a) A bright-field electron micrograph showing a narrow precipitate free zone at a grain boundary after ageing for 10 min at  $800^\circ\text{C}$ ; (b) a precipitate dark-field image of the same area showing enhanced precipitation of matrix-dot vanadium carbide near the precipitate free zone.

matrix-dot precipitation. The same effect is produced by quenching from  $1340^\circ\text{C}$  and ageing between  $800$  and  $925^\circ\text{C}$ . Such pfz have been reported for austenitic stainless steels by Silcock and Denham [2]. Dark-field micrographs using vanadium carbide reflections showed that the precipitates in the enhanced zone are of a similar size to those within the grain, but have a higher density, see Fig. 1b. A similar phenomenon occurs for vanadium carbide [2] and  $\text{M}_{23}\text{C}_6$  precipitation in austenite [11].

Vacancies are known to be important in the nucleation of matrix-dot MC carbides [1] and the formation of pfz has been explained previously [2] in terms of grain boundaries acting as vacancy sources during ageing. However, if this were to occur relief of strain around particles close to the boundary would be expected. None was observed from measurement of strain field images [12, 13] of matrix-dot particles in agreement with the work of Froes and Warrington on TaC in austenite [14].

We wish to propose an alternative mechanism involving the vacancy-induced solute segregation process first described by Aust *et al.* [15] and recently observed by Bercovici *et al.* [16]. The grain boundary acts as a vacancy sink during the quench, producing a vacancy concentration gradient in its vicinity (Fig. 2). If there is a high binding energy between vacancies and solute, as suggested by Silcock and Denham [2], the generation of this vacancy profile will entail a flux of vacancy/solute complexes towards the boundary [17]. During this process collisions may occur, which may release vacancies to the

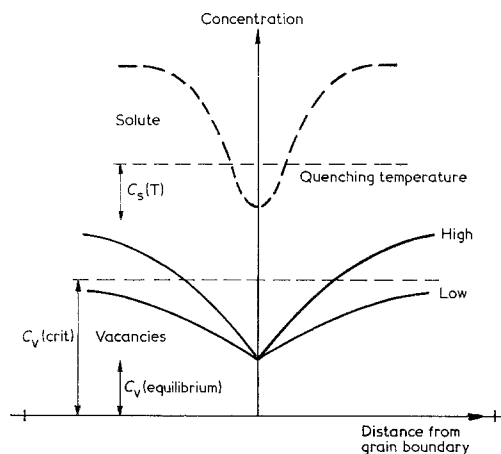


Figure 2 The vacancy (solid lines) and solute (dashed line) profiles adjacent to a grain boundary immediately after quenching.

boundary, leaving behind a less mobile cluster. Subsequent encounters with other solute/vacancy pairs can lead to growth of the clusters and formation of precipitate in the pez.

The above model is consistent with the present observations. After low temperature solution treatment a pre-age has been found necessary for the formation of pez, as only under these conditions is a sufficient solute supersaturation available for the formation of large numbers of solute/vacancy pairs and complexes. The critical nucleus size will also be smaller at lower ageing temperatures. However, in specimens quenched from 1340°C a higher solute supersaturation exists and the formation of pez occurs at higher ageing temperatures ( $\geq 800^\circ\text{C}$ ). Here the diffusion rate of clusters towards the boundary will be higher leading to a greater flux of solute and a higher probability of nucleation in this region before general bulk matrix-dot precipitation removes the solute and vacancy supersaturations. There will be a narrow pfz because of the presence of a solute depleted zone caused by grain-boundary precipitation. Observations of similar enhanced zones of NbC precipitates in austenite, which is neutron irradiated during ageing [18], may also be readily explained on the basis of solute/vacancy pair migration towards grain boundaries.

The operation of the grain boundary as a sink for vacancies during the quench also explains the occurrence of relatively wide pfz on ageing above 600°C, using the approaches outlined by other workers for aluminium alloys [19-21]. Thus during, and for a short time after the quench, a vacancy profile will be established adjacent to grain boundaries which act as vacancy sinks. The slope of this profile will be dependent on both homogenizing temperature and quenching speed (solid lines in Fig. 2). Superimposed on this will be a narrower solute concentration profile due to segregation to the grain boundary during the quench (dashed line in Fig. 2). On ageing at 600°C and above, nucleation can occur near the boundary until the point at which the vacancy concentration falls below that necessary to enable precipitation  $C_v(\text{crit})$ , i.e. a vacancy depleted zone forms. Thus the wide pfz is essentially vacancy depleted while the narrow one is solute depleted. This explanation presumes that the temperature at which homogeneous nucleation can occur without excess vacancies is  $\sim 500$  to  $550^\circ\text{C}$ .

### 3.2. Secondary precipitation

A further type of precipitate (see Fig. 3a) with a maximum density  $\sim 7 \times 10^{14} \text{ cm}^{-3}$ , was observed in the temperature range 600 to 925°C after long ageing times (e.g.  $> 12 \text{ h}$  at  $700^\circ\text{C}$ ). Simultaneously extra spots, which cannot be accounted for by the cube/cube orientation relationship of the matrix-dot precipitate, [9] appeared in electron diffraction patterns. Trace analysis of precipitate dark-field micrographs showed that most of the precipitates were large plates  $\sim 30 \text{ nm}$  in diameter and lying on  $\{111\}$  habit planes with sides parallel to  $\langle 112 \rangle$  directions, but a small fraction lay on  $\{100\}$  planes. During continued ageing these precipitates coarsened rapidly from  $\sim 30$  to  $\sim 200 \text{ nm}$  in diameter after 500 h at  $700^\circ\text{C}$  (Fig. 3b). In contrast the diameter of the matrix-dot particles only increased from 8 to 15 nm during this ageing treatment. On ageing, the density of dislocations in the matrix increases rapidly, probably as a result of prismatic punching from the growing particles. The form of these plates is similar to "the isolated site stacking fault precipitates" reported by Silcock [22], who suggested that these are nucleated at dislocations punched from the growing matrix-dot. However, in the present case there is no evidence for either this process or nucleation on matrix-dot particles.

Selected-area diffraction patterns taken from large individual plates  $\sim 100 \text{ nm}$  in diameter showed two equally-spaced superlattice reflections between the transmitted beam and the  $\{220\}$  fundamental reflections, identical to those reported for ordered  $\text{V}_6\text{C}_5$  [23]. Precipitate dark-field micrographs taken using the superlattice reflections showed the fine domain structure of the precipitates (Fig. 3c). Thus it is concluded that this secondary type of precipitation is  $\text{V}_6\text{C}_5$ , and the lattice parameter measured from electron diffraction patterns is 0.415 nm compared with the matrix 0.352 nm.

The orientation relationships between the vanadium carbide plates and the matrix have been determined using selected-area diffraction from individual or small numbers of precipitates, and are close to those shown below.

- (a)  $(111)_{\text{matrix}} // (112)_{\text{V}_6\text{C}_5}$   
 and  $[2\bar{2}0]_{\text{matrix}} // [\bar{1}\bar{1}1]_{\text{V}_6\text{C}_5}$  (3.4%)  
 $[\bar{2}\bar{2}4]_{\text{matrix}} // [\bar{2}20]_{\text{V}_6\text{C}_5}$  (2.4%)  
 $[0\bar{2}2]_{\text{matrix}} // [\bar{3}11]_{\text{V}_6\text{C}_5}$  (0.7%)
- (b)  $(100)_{\text{matrix}} // (111)_{\text{V}_6\text{C}_5}$   
 and  $[002]_{\text{matrix}} // [0\bar{2}2]_{\text{V}_6\text{C}_5}$  (16%)  
 $[020]_{\text{matrix}} // [4\bar{2}\bar{2}]_{\text{V}_6\text{C}_5}$  (3.5%)

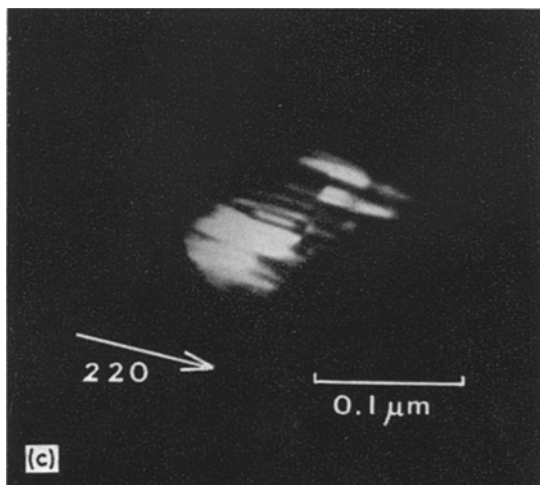
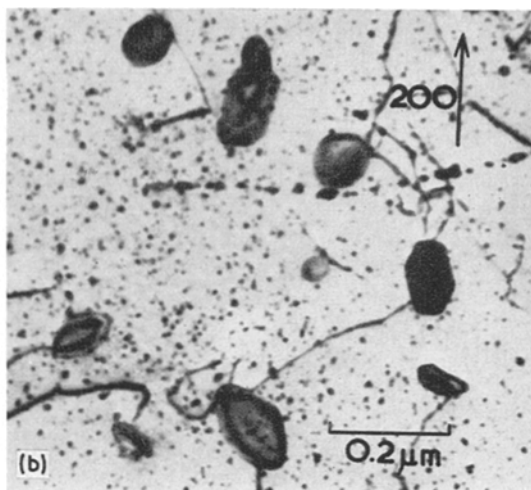
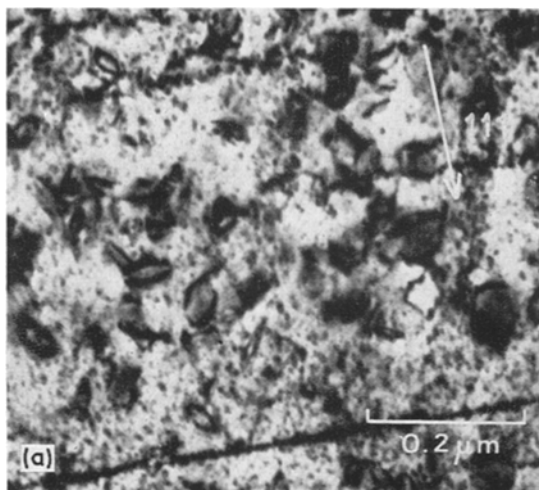


Figure 3 Secondary vanadium carbide precipitation (a) in the early stages of growth and (b) after considerable coarsening. The ordered domains (c) of the  $V_6C_5$  structure are revealed in a precipitate dark-field image formed with a superlattice reflection.

where for convenience the  $V_6C_5$  phase is indexed in terms of the fundamental sodium chloride vanadium carbide lattice. The percentages in brackets indicate the misfit in the directions shown.

Compared with the matrix-dot precipitate, which has cube/cube orientation relationship (misfit  $\sim 15\%$ ) the  $V_6C_5$  has much lower misfit in the habit plane. The late occurrence of the  $V_6C_5$  in the ageing sequence may thus be interpreted in terms of difficulty in nucleation compared with the matrix dot form.

#### 4. Conclusions

Ageing of this alloy in the temperature range 600 to 925°C produces grain-boundary precipitate, together with matrix-dot and sometimes stacking-fault precipitate, depending upon time

and temperature. At long ageing times, secondary precipitation of  $V_6C_5$  plates occurs.

Both matrix-dot precipitate free and enhanced zones are formed, depending upon ageing conditions. The latter is explained in terms of vacancy induced segregation of solute towards grain boundaries.

#### Acknowledgements

Most of this work was carried out in the Brown Boveri Research Centre, Baden, Switzerland, during a research studentship held by RBS. The financial support of this company is gratefully acknowledged.

#### References

1. F. H. FROES, D. H. WARRINGTON and R. W. K. HONEYCOMBE, *Acta Met.* **15** (1967) 157.
2. J. M. SILCOCK and A. W. DENHAM, in "The Mechanism of Phase Transformations in Crystalline Solids" (Institute of Metals, London, 1969) 59.
3. R. B. SCARLIN, G. E. HOLLOX and J. W. EDINGTON, *J. Mater. Sci.* **6** (1971) 1322.
4. L. K. SINGHAL and J. W. MARTIN, *Trans. Met. Soc. AIME* **242** (1968) 815.
5. F. H. FROES, M. G. H. WELLS and B. R. BANERJEE, *Met. Sci. J.* **2** (1968) 232.
6. V. RAMASWAMY, P. R. SWANN and D. R. F. WEST, VIIth International Conference on Electron Microscopy, Grenoble (1970) p. 543.
7. *Idem*, in "Electron Microscopy and Structure of Materials", Proceedings of 5th International

- Materials Symposium, University of California Press, Berkeley (1972).
8. J. L. KAAE and T. D. GULDEN, *Trans. Met. Soc. AIME* **245** (1969) 1832.
  9. R. B. SCARLIN and J. W. EDINGTON, *Metal Sci. J.* **7** (1973) 208.
  10. J. M. SILCOCK and W. J. TUNSTALL, *Phil. Mag.* **10** (1964) 361.
  11. G. R. KEGG and J. M. SILCOCK, CEBG Report RD/L/N75/71 (1971) 20.
  12. M. F. ASHBY and L. M. BROWN, *Phil. Mag.* **8** (1963) 1083.
  13. *Idem*, *ibid* **8** (1963) 1649.
  14. F. H. FROES and D. H. WARRINGTON, *Trans. Met. Soc. AIME* **245** (1969) 2009.
  15. K. T. AUST, R. E. HANNEMAN, P. NIESSEN and J. H. WESTBROOK, *Acta Met.* **16** (1968) 291.
  16. S. J. BERCOVICI, C. E. L. HUNT and P. NIESSEN, *J. Mater. Sci.* **5** (1970) 326.
  17. T. R. ANTHONY, *Acta Met.* **17** (1969) 603.
  18. J. P. SHEPHERD, *Met. Sci. J.* **3** (1969) 229.
  19. D. W. PASHLEY, M. H. JACOBS and J. T. VIETZ, *Phil. Mag.* **16** (1967) 51.
  20. M. H. JACOBS and D. W. PASHLEY, in "The Mechanism of Phase Transformations in Crystalline Solids" (Institute of Metals, London, 1969) p. 43.
  21. P. N. T. UNWIN, G. W. LORIMER and R. B. NICHOLSON, *Acta Met.* **17** (1969) 1363.
  22. J. M. SILCOCK, *ibid* **14** (1966) 687.
  23. J. D. VENABLES, D. KAHN and R. G. LYE, *Phil. Mag.* **18** (1968) 177.

Received 19 October 1973 and accepted 8 April 1974.